

Thermal and Electrical Properties of Nanocomposites of Reduced Graphene Oxide and Silver Nanoparticles

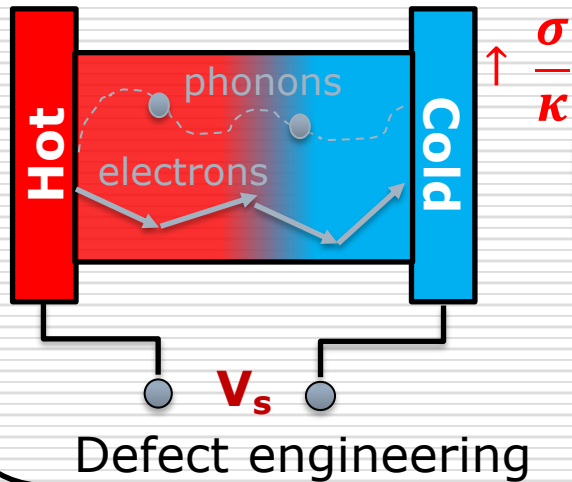
Archana Tiwari

Department of Physics
Banaras Hindu University

archana.tiwari@bhu.ac.in

Motivation: Thermoelectric applications

Thermal and electron transport



$$ZT = \frac{\sigma}{\kappa} TS^2$$

Band gap opening

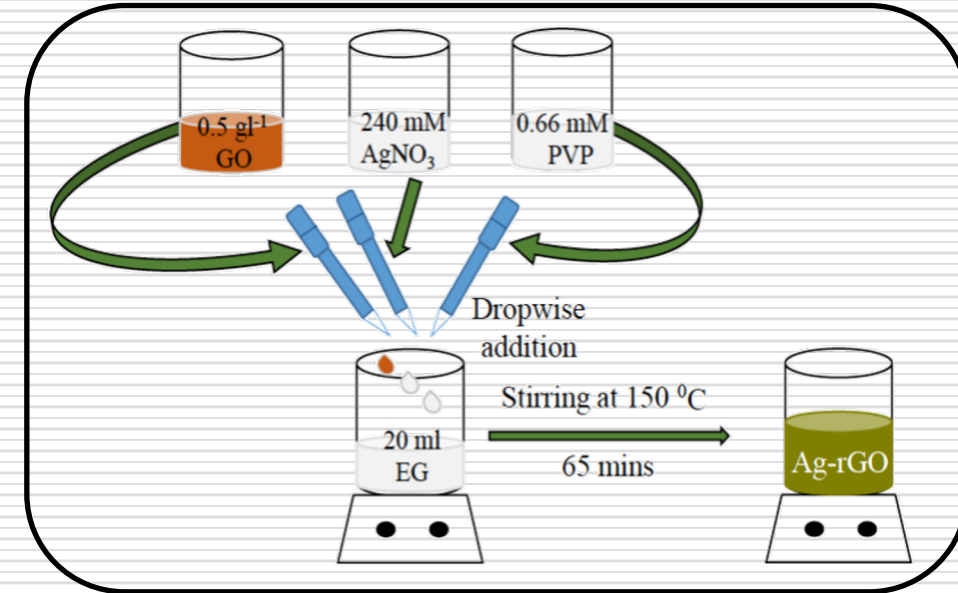
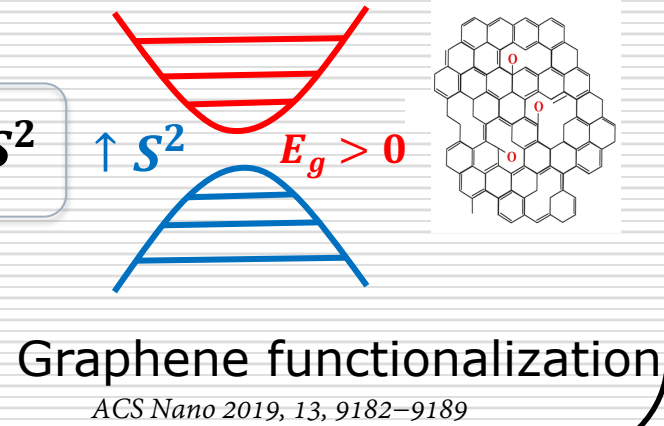


Fig 1: Schematic illustration of thermal and electron transport.

Fig 2: Schematic illustration: synthesis of Ag-rGO.

Prerequisites for efficient thermoelectric materials:

1. High electrical conductivity (σ): Graphene ($\sim 10^4$ S/m)
2. High Seebeck coefficient (S): Graphene functionalization and bandgap opening ($127\text{--}287$ $\mu\text{V K}^{-1}$)
3. Low thermal conductivity (κ): Defect/dopants and phonon scattering (0.1 W/mK)

Results: Spectroscopic characterization

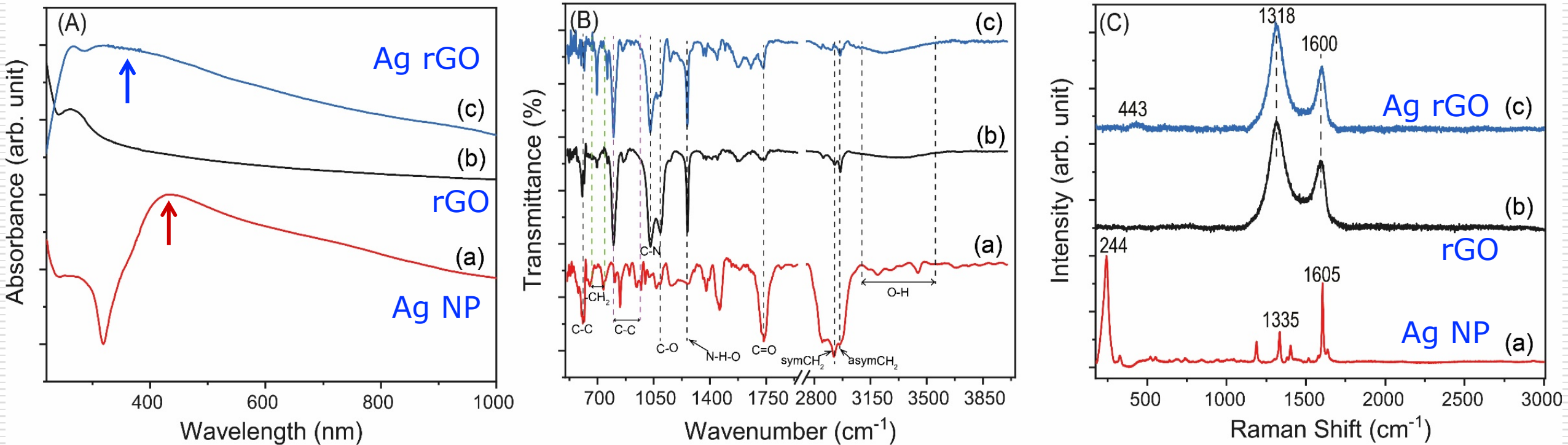


Fig 3: (A) UV-vis absorption spectra, (B) FTIR spectra and (C) Raman spectra for (a),(b) and (c) which respectively correspond to Ag NP, rGO and Ag-rGO.

✓ I_D/I_G ratio is found to be 1.6(2) for rGO and 1.7(5) for Ag-rGO.

Results: Size and Structure

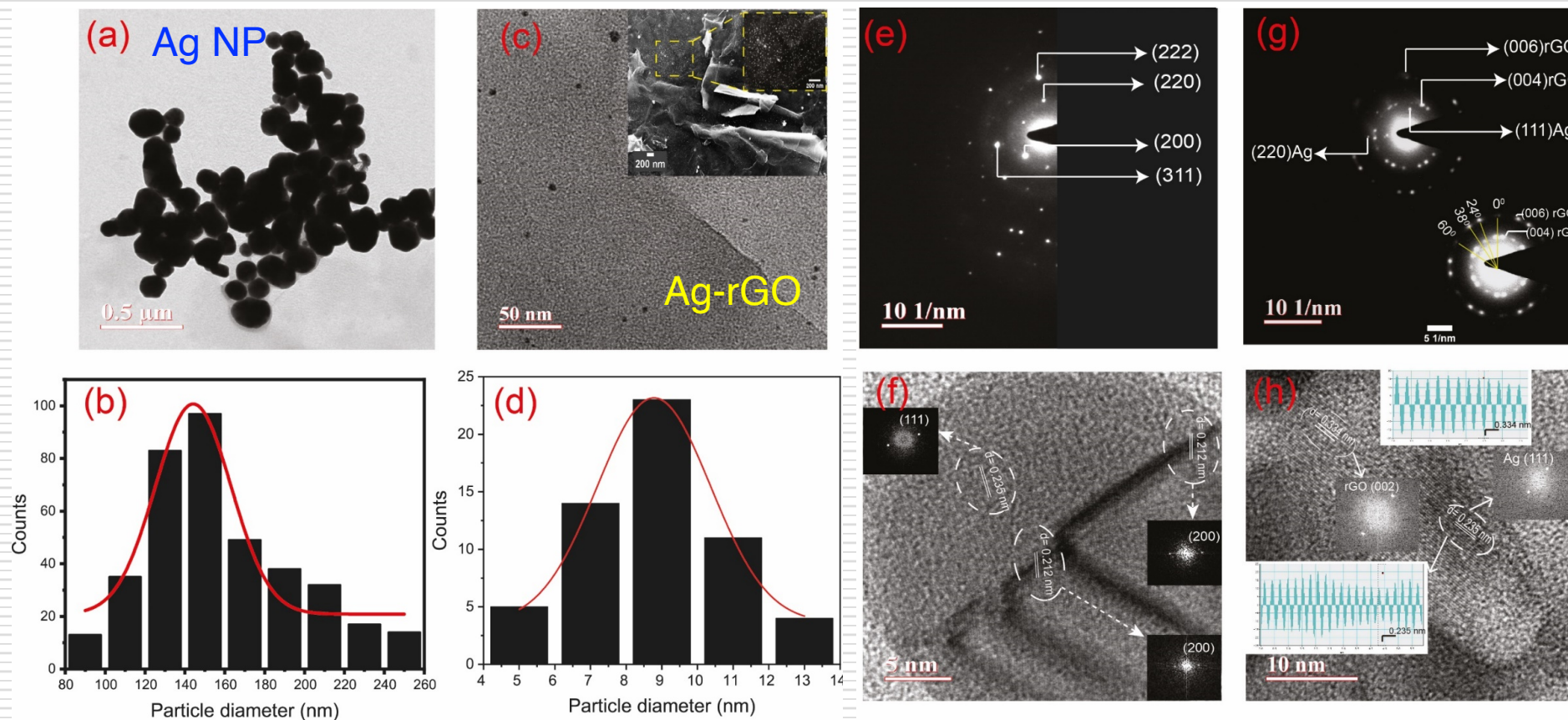
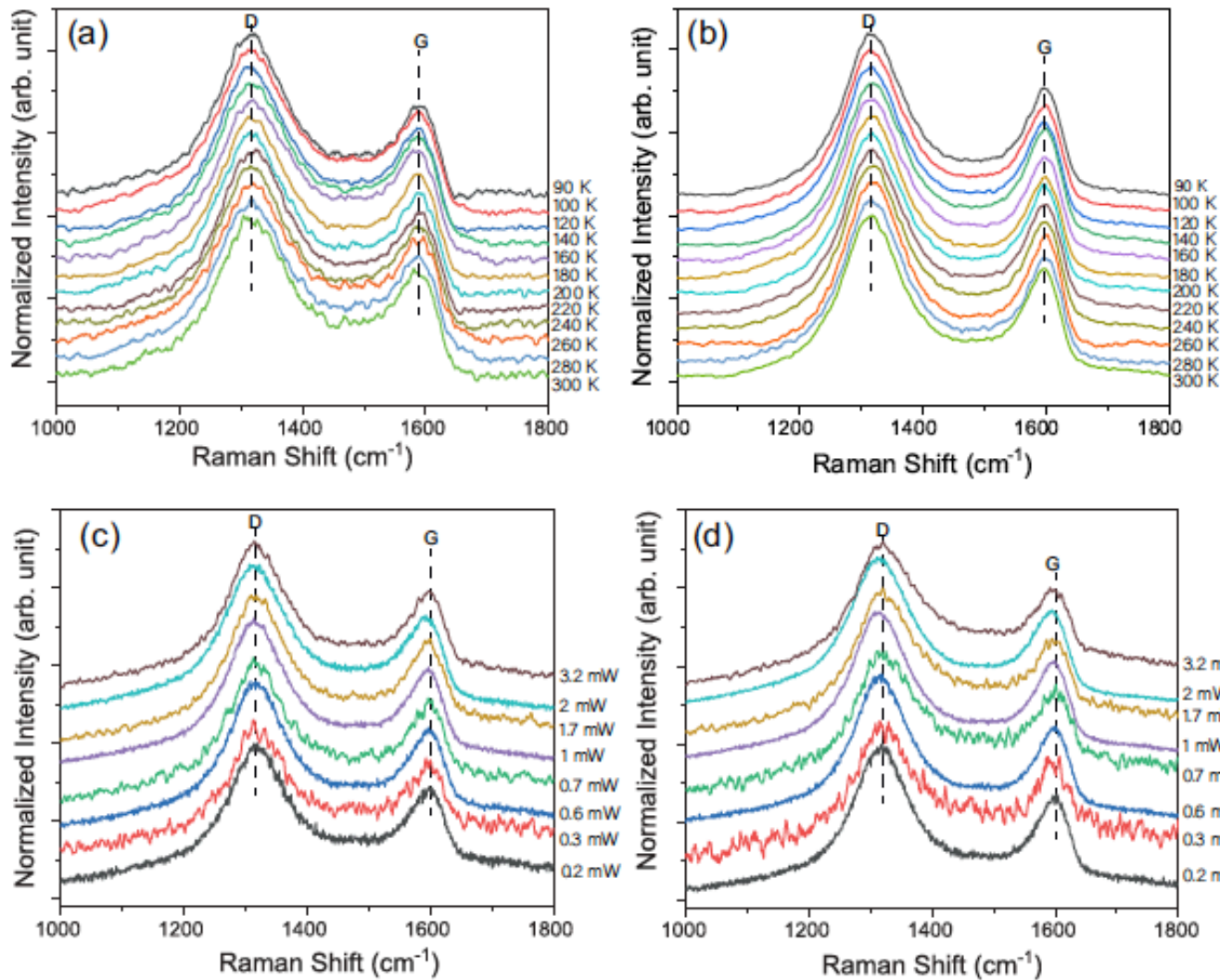


Fig 4: (a), (c) TEM micrographs of Ag NP and Ag-rGO nanocomposite, (b), (d) refer to their corresponding particle size distribution, (e), (g) SAED pattern of Ag NP and Ag-rGO where inset shows angle between the spots corresponding to rGO plane and (f), (h) are their HRTEM micrographs.

- ✓ Simultaneous reduction of Ag and GO leads to formation of smaller sized NP in our study, possibly **due to attachment of Ag⁺ ions with carboxylated carbonaceous fragments present in GO obtained during Hummers method.**
- ✓ **The angle between 3 spots with respect to a reference spot is found to be 24 , 38 and 60° as shown in inset of Fig.(g).**
- ✓ These spots are related to turbostratic layered arrangement of graphene.

Results: Raman thermometry



Variation in Raman frequency with T is related to anharmonic components in lattice potential energy such as thermal expansion and conduction

Thermal variation in Raman frequency $\omega(T)$

$$\omega(T) = \omega_0 + \chi_T T$$

Linear power dependence of ω

$$\frac{\partial \omega}{\partial P} = \chi_P$$

G-band	χ_T (cm ⁻¹ K ⁻¹)	χ_P (cm ⁻¹ mW ⁻¹)
rGO	-0.014	-0.571
Ag-rGO	-0.012	-0.657

Fig 5: Temperature dependent Raman spectra for (a) rGO and (b) Ag-rGO. Power dependent Raman spectra for (c) rGO and (d) Ag-rGO.

Results: Thermal and electrical conductivity

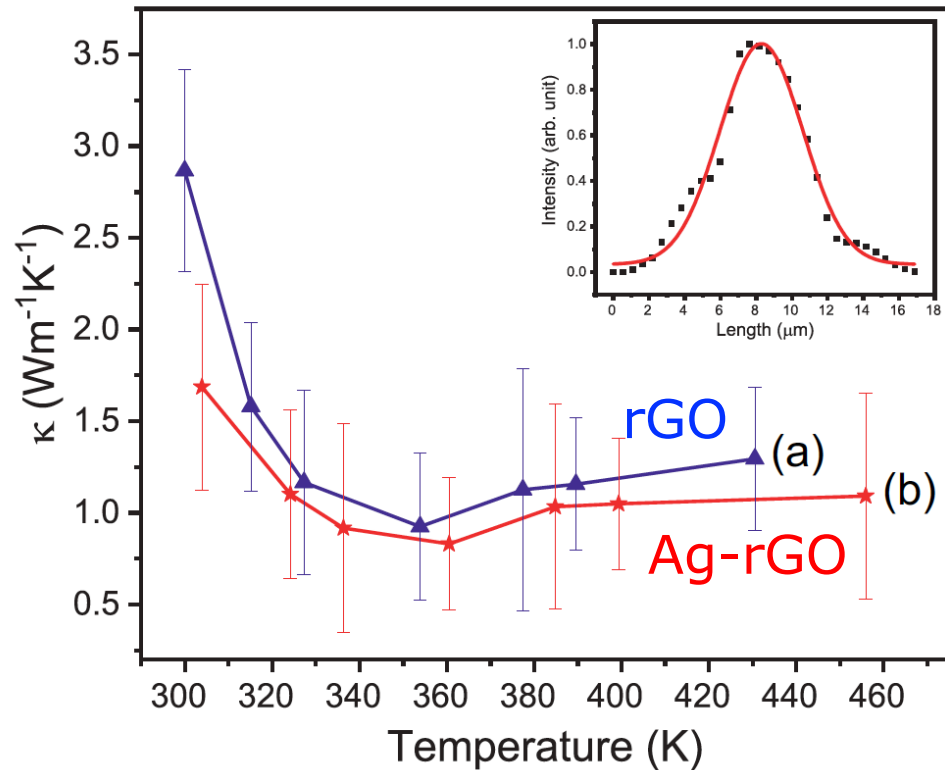


Fig 6: Variation of κ with temperature for (a) rGO and (b) Ag-rGO. Inset shows beam profile of 785 nm laser on sample's surface.

- ✓ For rGO and Ag-rGO at 0.3 mW laser power (dT at 6 K and 10 K), κ are found to be 2.86(1) and 1.69(1) $\text{Wm}^{-1}\text{K}^{-1}$ respectively.

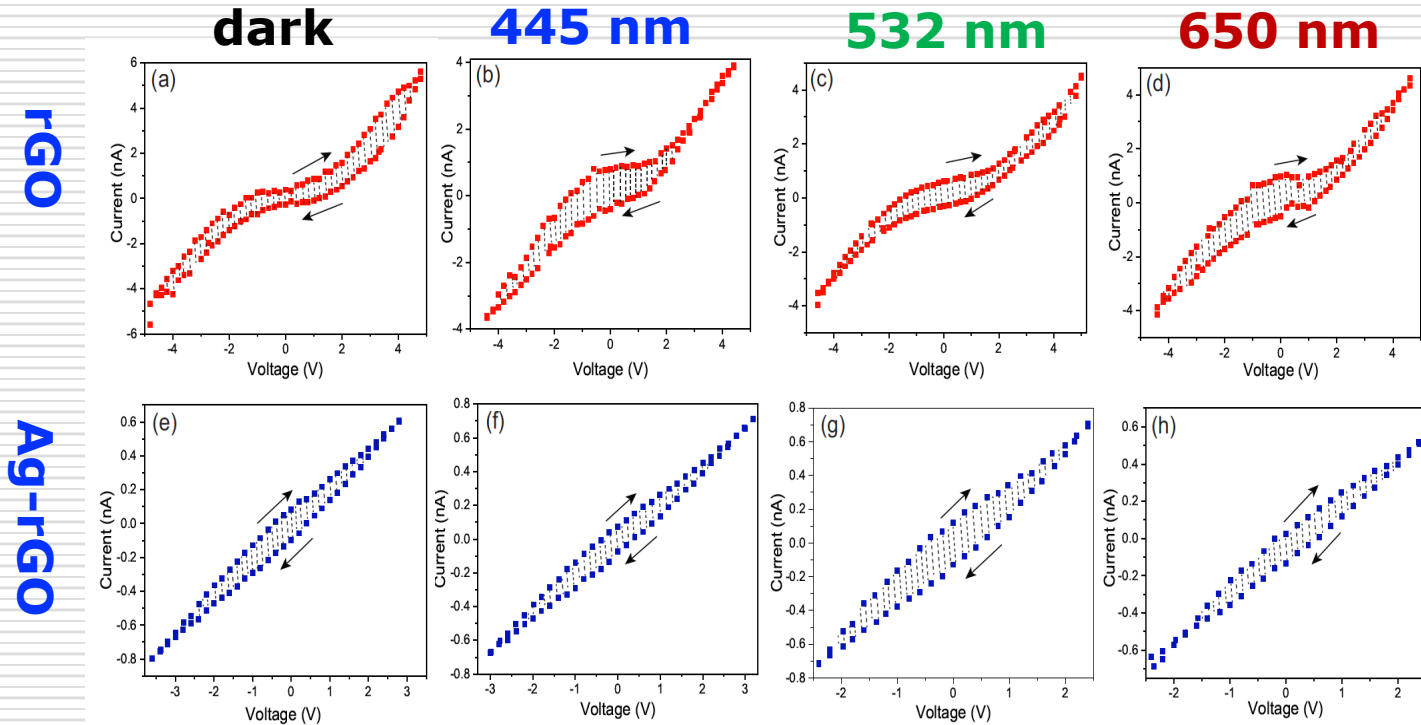


Fig 7: I-V curves obtained while illuminating the sample under different excitation wavelength for rGO: (a) dark, (b) 445 nm, (c) 532 nm, (d) 650 nm and Ag-rGO: (e) dark, (f) 445 nm, (g) 532 nm, (h) 650 nm.

- ✓ Upon illumination, in LSPR of Ag NP, it can improve the EM field in their immediate vicinity resulting in improvement in absorption of light thereby generating light-induced electron-hole pairs.

Conclusion and prospects

- * Anharmonicity, thermal expansion and thermal conductivities are examined for rGO, Ag-rGO
- * Thermal conductivities of rGO and Ag-rGO at ~ 300 K are $2.86(1) \text{ Wm}^{-1}\text{K}^{-1}$ and $1.69(1) \text{ Wm}^{-1}\text{K}^{-1}$ respectively.
- * I-V hysteresis loops show variation in space charges and electrical resistances in presence and absence of **plasmonic** excitations.
- * Low thermal conductivity in turbostratic graphene plus photo tunable electrical conductance offer potential applications in fabrication of **photo-thermoelectric devices, plasmon-enhanced opto-electronic device, photodetector etc.**

References

- Li, Q.Y., Feng, T., Okita, W., Komori, Y., Suzuki, H., Kato, T., Kaneko, T., Ikuta, T., Ruan, X. and Takahashi, K., 2019. Enhanced thermoelectric performance of as-grown suspended graphene nanoribbons. *ACS nano*, 13(8), pp.9182-9189.
- Chettri, P., Vendamani, V.S., Tripathi, A., Pathak, A.P. and Tiwari, A., 2016. Self assembly of functionalised graphene nanostructures by one step reduction of graphene oxide using aqueous extract of *Artemisia vulgaris*. *Applied Surface Science*, 362, pp.221-229.
- Sharma, M., Rani, S., Pathak, D.K., Bhatia, R., Kumar, R. and Sameera, I., 2021. Temperature dependent Raman modes of reduced graphene oxide: Effect of anharmonicity, crystallite size and defects. *Carbon*, 184, pp.437-444.
- Cançado, L.G., Takai, K., Enoki, T., Endo, M., Kim, Y.A., Mizusaki, H., Jorio, A., Coelho, L.N., Magalhães-Paniago, R. and Pimenta, M.A., 2006. General equation for the determination of the crystallite size L_a of nanographite by Raman spectroscopy. *Applied Physics Letters*, 88(16), p.163106.
- Calizo, I., Balandin, A.A., Bao, W., Miao, F. and Lau, C.N., 2007. Temperature dependence of the Raman spectra of graphene and graphene multilayers. *Nano letters*, 7(9), pp.2645-2649.
- Gurung, S., Arun, N., Pathak, A.P., Nelamarri, S.R., Tripathi, A. and Tiwari, A., 2023. *Journal of Materials Science: Materials in Electronics*, 34(13), p.1108.

Acknowledgement

Sweta Gurung

Ajay Tripathi

Sikkim University

Anand Pathak
Arun Nimmala

Hyderabad University

Srinivasa R Nelamari

MNIT Jaipur

ECRA-SERB

IoE BHU

IUAC, New Delhi